PNAS nexus

Main Manuscript for

Revisiting immunity versus exposure in schistosomiasis: a mathematical modelling study of delayed concomitant immunity

Gregory C. Milne[1,2,†], Rebecca C. Oettle[3,†], Charles Whittaker[2,4], Narcis B. Kabaterine[5], Maria-Gloria Basáñez[2,4], Joanne P. Webster[1,2], Martin Walker[1,2,*], Shona Wilson[3,*]

[*] Martin Walker, Department of Pathobiology and Population Sciences, Royal Veterinary College, United Kingdom

[*] Shona Wilson, Department of Pathology, University of Cambridge, Cambridge, United Kingdom.

[†] Equal contributions

1. Department of Pathobiology and Population Sciences, Royal Veterinary College, Hatfield, United Kingdom.
2. London Centre for Neglected Tropical Disease Research, Department of Infectious Disease Epidemiology, School of Public Health, Imperial College London, London, United Kingdom.
3. Department of Pathology, University of Cambridge, Cambridge, United Kingdom.
4. MRC Centre for Global Infectious Disease Analysis, Department of Infectious Disease Epidemiology, School of Public Health, Imperial College London, London, United Kingdom.
5. Vector Control Division, Ugandan Ministry of Health, Kampala, Uganda.

Email: mwalker@rvc.ac.uk; sw320@cam.ac.uk

Author Contributions: Conceptualization: RCO, MGB, MW and SW; Investigation (data collection): RCO, NBK and SW; Methodology: GCM, RCO, CW and MW; Formal analysis: GCM and RCO; Supervision: JPW, MW and SW; Funding Acquisition: JPW, MW and SW; Writing – Original Draft Preparation: GCM and MW; Writing – Review & Editing: all authors.

Competing Interest Statement: Authors declare no competing interest.

Classification: Biological Sciences (Population Biology).

Keywords: schistosomiasis, adaptive immunity, public health, modelling, praziquantel.

This PDF file includes:

Main Text

Abstract

The relative contributions of exposure versus acquired immunity to the epidemiology of human schistosomiasis has been long debated. While there is considerable evidence that humans acquire partial immunity to infection, age- and sex-related contact patterns with water bodies contaminated with infectious cercarial schistosome larvae also contribute to typical epidemiological profiles of infection. Here, we develop a novel schistosome transmission model that incorporates both partially protective 'delayed concomitant' acquired immunity—stimulated by dying worms—and host age- and sex-dependent patterns of exposure. We use a contemporary Bayesian approach to fit the model to historical individual data on exposure to infectious cercaria, eggs per gram of faeces (epg), and immunoglobulin E (IgE) antibodies specific to *Schistosoma mansoni* Tegumental-Allergen-Like protein 1 (SmTAL1) collected from a highly endemic community in Uganda, estimating the relative contributions of exposure and acquired immunity. We find that model variants incorporating or omitting delayed concomitant immunity describe equally well the age- and sex-specific immunoepidemiological patterns observed before intervention and 18 months after treatment. Over longer time-horizons, we find that acquired immunity creates subtle differences in immunoepidemiological profiles during routine mass drug administration that may confer resilience against elimination. We discuss our findings in the broader context of the immunoepidemiology of schistosomiasis.

Significance Statement

A longstanding question in schistosome epidemiology is the relative contributions of exposure and immunity to observed age-infection profiles. Previous attempts to disentangle these processes have been hampered by a lack of paired data on markers of exposure, infection, and immunity. Furthermore, most studies have assumed immunostimulation by living adult worms—not dying worms, for which there is currently the most compelling evidence. To combat these limitations, here we collate a unique dataset comprising individual-level data on cercarial exposure, infection intensity, and IgE antibodies stimulated by an antigen (SmTAL1) released upon death of adult *Schistosoma mansoni*. We use these data to calibrate a novel mathematical model, allowing for robust inference on the relative contributions of exposure and immunity.

Introduction

Schistosomiasis is a parasitic neglected tropical disease (NTD) of considerable public health importance. Schistosomiasis affects approximately 240 million people worldwide[1], causing chronic and acute morbidity, including anaemia, wasting, and damage to intestinal or urogenital systems. The global burden of schistosomiasis was estimated in 2021 at 1.75 (95% Uncertainty Interval, UI, 1.04–2.99) million disability adjusted life years, with 12,900 deaths (95% UI 11,400–14,700), the majority of which occurred in sub-Saharan Africa[2]. The World Health Organization (WHO) has targeted schistosomiasis for elimination as a public health problem (<1% prevalence of heavy-intensity infections) by 2030, principally using a strategy of annual or semi-annual mass drug administration (MDA) with praziquantel[1].

Schistosomes are transmitted indirectly via intermediate freshwater snail hosts; consequently, exposure is linked to contact with water bodies containing infectious cercarial larvae. Five decades ago, Warren[3] first noted the difficulty of distinguishing the contributions of "immunology or ecology" to the convex age-intensity profiles of schistosome infections[4]. Repeated exposure may promote a partially protective immune response, causing peak infection intensity to occur in earlier childhood in areas of intense transmission due to the more rapid acquisition of immunity ('peak shift')[5–8]. However, childhood peaks in infection intensity are also likely driven by age-dependent contact rates with contaminated water bodies, which are often greater in children than adults[9,10]. Hence, the relative importance of acquired immunity ("immunology") versus exposure ("ecology") to the epidemiology of schistosomiasis has remained elusive.

Resolving the contributions of immunity and exposure is critical for understanding the transmission dynamics of schistosomiasis and for modelling responses to interventions. Protective immunity increases the resilience of helminthiases to intervention, making it more difficult to achieve elimination targets[9,11]. Recent advances have indicated that immunoglobulin E (IgE) responses against Tegumental-Allergen-Like (TAL) proteins are likely a major component of so-called 'delayed concomitant immunity'[12]. By this proposed mechanism, protective immunological responses are mediated by the death of adult schistosomes which induce antibodies that are cross-reactive with TAL proteins present on invading cercariae[12,13]. Delayed concomitant immunity may also provide a strong passive vaccination effect following praziquantel treatment of heavily infected individuals, initially boosting immunity and enhancing protection against re-infection[14], but waning following subsequent treatments.

In recent years, schistosomiasis transmission models have been increasingly used for public health decision-making, including on the frequency and population coverage of MDA required to achieve the 2030 elimination goals (reviewed previously[15]). However, due to uncertainty on the relative contributions of exposure versus immunity, these models have typically attributed age-infection patterns exclusively to exposure (e.g.[16], although see also[9–11,17,18]). Depending on the nature and strength of acquired immunity, this assumption may make current projections on the

long-term effectiveness of MDA too optimistic. Improved understanding of acquired immunity in natural populations would also benefit the development of effective schistosomiasis vaccines [19,20].

Here, we develop a novel mathematical transmission model to resolve the contributions of exposure and acquired immunity to the epidemiology of intestinal schistosomiasis using a unique immunoepidemiological dataset collected from 110 individuals aged between 7 and 50 years living on the shores of Lake Albert, Uganda, before the initiation of MDA [21,22]. We use data on water-contact and malacological surveys [23,24] to infer age- and sex-dependent patterns of cercarial exposure and estimate the protective effect of delayed concomitant immunity using individual-level parasitological data on infection intensity and immunological data on *Schistosoma mansoni* TAL1 (SmTAL1) IgE antibodies. We compare model variants with and without protective acquired immunity to determine its importance in capturing observed immunoepidemiological profiles. We also explore how immunity affects transmission dynamics during MDA. We discuss our findings in the context of the longstanding debate on schistosome exposure versus immunity and the broader immunoepidemiology of schistosomiasis.

Results

Cercarial exposure shows a similar convex-like pattern in males and females, peaking at 11 and 15 years, respectively, before gradually declining throughout adulthood (Figure 1). The fit of the transmission model (Figure 2) to pre-intervention immunoepidemiological data is shown in Figure 3A and 3B ('Baseline') for the model variant without protective immunity ('standard model') and with protective immunity ('immunity model'). The immunity model shows a sharper peak in infection intensity (eggs per gram of faeces, epg) in school-aged children (SAC) and a steeper decline into older ages than the standard model (Figure 3A, 'Baseline'; see Supporting Information Fig. S2 for an overlaid plot). Accordingly, in older ages the rate of increase in SmTAL1-IgE optical density (OD) is lower for the immunity model than for the standard model (Figure 3B, 'Baseline'). The deviance information criterion (DIC) indicates the standard model to be a more parsimonious and adequate fit to the data than the more complex immunity model (standard model 50.94 (95% credible interval, crI, 50.67–51.44), immunity model 51.12 (95% crI 50.73–51.59)).

Parameter posterior distributions from each model are summarized in Figure 4 (see also Supporting Information Fig. S3 and S4; Fig. S5 and S6 for pairwise correlations, and Fig. S7 for posterior log likelihoods). The median SmTAL1-IgE half-life ($12\ \ln(2)\ /\sigma$, where σ is the rate of loss; Figure 4) is 1.1 months for both models, with 95% crIs of 1.0–1.6 months for the standard model and 1.0–1.5 months for the immunity model. For the immunity model, the strength of protection against cercarial infection establishment is highly uncertain (ω, posterior distribution uniform over prior range; Figure 4, Supporting Information Fig. S4) despite mild and statistically non-significant pairwise correlations with other fitted parameters (correlation coefficient range -0.15 to 0.11, Supporting Information Fig. S6). Some resolution was obtained for the human-to-snail population

density parameter (N_1/N_2, greater posterior vs. prior densities for values over ~0.3; Figure 4, Supporting Information Fig. S3 and S4), but other parameter posterior estimates were largely indistinguishable from priors (Figure 4).

Both model variants show good predictive performance against epg and SmTAL1-lgE OD values collected at 5 weeks (Figure 3A, 3B, '5 weeks') after praziquantel treatment and against epg collected additionally at 12 months (Figure 3A, '12 months'), and 18 months (Figure 3A, '18 months') post-treatment (note that SmTAL1-lgE was only measured up to 5 weeks after treatment)[24]. There was no difference in model performance by root mean squared error in capturing post-treatment epg (standard model, 255 (95% crI 47.3–617); immunity model, 260 (95% crI 47.7–628)) or SmTAL1-lgE (standard model, 0.24 (95% crI 0.18–0.34); immunity model, 0.23 (95% crI 0.17–0.32)) (Supporting Information Fig. S8).

The long-term epg dynamics through 10 rounds of annual MDA—assuming 75% coverage of SAC[1] and a nominal 30% of adults (≥16 years old), yielding a mean coverage of 50.5% in line with Ugandan coverage surveys[25,26]—are consistently lower for the immunity model compared to the standard model (Figure 3C, 'epg'), likely since infection intensities are more concentrated in SAC in the former (Figure 3A, 'Baseline'). SmTAL1-lgE OD dynamics are similar in both models until approximately 5 years after MDA initiation, after which antibodies decline faster in the immunity model (Figure 3C, 'SmTAL1-lgE (OD)'), reflecting a lower antigenic stimulus from lowered worm burdens (and, consequently, epg; Figure 3C). For both models, SmTAL1-lgE ODs fall below pre-intervention levels (Figure 3C). The immunity model projections are associated with wide uncertainty intervals, particularly for epg (Figure 3C), reflecting uncertainty in both pre-intervention fits (chiefly in SAC; Figure 3A, 'Baseline') and the strength of protection afforded by SmTAL1-lgEs (ω, Figure 4). This translates into more uncertain prevalence dynamics for the immunity model, further compounded by uncertainty in the among-host worm overdispersion parameter (k, used to calculate prevalence; Supporting Information Fig. S9).

Some immunity model simulations initially show stark epg decreases which thereafter remain persistently low (Figure 3C 'epg', immunity model lower 95% crI). These are associated with low values of basic reproduction number (R_0), human-to-snail population density (N_1/N_2), SmTAL1-lgE decay (σ), and immune constant (ϕ), and high values of immune protection (ω) (Supporting Information Fig. S10).

Discussion

The relative importance of age-dependent exposure versus acquired immunity to typical convex age-intensity profiles is a major unresolved question in schistosomiasis epidemiology[3,9–11,27]. Understanding the relative contributions of these two processes has important implications for transmission dynamics, responses to MDA, including the feasibility of achieving the WHO 2030 goals[1]. Here, we have used a unique immunoepidemiological dataset[24]—which includes individual

data on exposure to infectious cercariae[23]—combined with a mathematical transmission model to attempt to resolve the effects of delayed concomitant immunity and age-dependent exposure on the epidemiology of intestinal schistosomiasis in a highly endemic region of western Uganda. We found that the model variants incorporating or omiting acquired immunity captured equally well observed age profiles of infection intensity and SmTAL1-IgE antibodies before and up to 18 months after praziquantel treatment. It therefore appears that delayed concomitant immunity is not required to adequately describe the transmission of intestinal schistosomiasis in this highly endemic epidemiological setting and its protective effect is highly uncertain. However, we also stress that we have taken a conservative approach to parameter inference, that the protective effects of immunity may only become apparent over longer time horizons in populations subject to MDA, and that the proxy of immunity used is a necessary simplification of the proposed delayed concomitant mechanism[12]. We also emphasize that these conclusions are based on findings from a single highly endemic setting, using data from 110 individuals. It is conceivable that a larger sample size would be required to detect acquired immunity if its effects are relatively weak. Therefore, acquired immunity should not be entirely discounted from future modelling efforts aimed at projecting the effectiveness of interventions.

Many previous mathematical modelling studies have considered the role of acquired immunity on the epidemiology of schistosomiasis, but these have generally focused on the theoretical implications of immunity for control and elimination efforts[9–11,18]. While some models have been calibrated against exposure and infection data[9–11], data have typically been lacking on antibody responses, limiting inference on the role of immunity[3]. The key novelty of our study is the use of individual data on exposure, infection and immunological responses which permits, in principle, the relative contributions of exposure and immunity to be disaggregated. We focused on delayed concomitant immunity (as opposed to other postulated mechanisms of acquired immunity[28]) to align with the available immunological data on SmTAL1-IgEs which comprise the primary antibody response following the death of adult worms[13,14,17,29–32] and which have been previously associated with reduced rates of reinfection (e.g.[33] and references therein). Notwithstanding, SmTAL1-IgE is a proxy for a proposed immunity-generating process acting via TAL family members such as SmTAL3, SmTAL5 and SmTAL11, since SmTAL3/SmTAL5/SmTAL11 responders are known to be a subset of SmTAL1 responders[12,13,34]. SmTAL3 and SmTAL11 are expressed predominantly in adult worms, and IgE specific to these antigens is cross-reactive with SmTAL5[13] expressed on cercariae and early schistosomulae. Hence, while immunity is stimulated by worm death (i.e., ‘delayed’), the protective response is thought to be protective against invading stages (i.e., ‘concomitant’).

We found that most model parameters were only weakly identifiable from the data, such that many different parameter combinations could yield similar immunoepidemiological patterns that adequately captured the data. We deliberately chose a conservative approach to parameter

inference by assigning vague priors to all unknown parameters and avoided harder assumptions associated with fixing values to uncertain model parameters. While this avoids potential bias, it also highlights the limitations and challenges of parameter inference using transmission models with multiple unknown or highly uncertain parameters[35]. The data were most informative on the half-life of SmTAL1-IgE antibodies, with both model variants yielding a central estimate of 1.1 months and an uncertainty range of 1–1.6 months. Without replacement, IgE has a circulating half-life of 2 days, and a half-life in the skin, the proposed site of parasite killing, of 16–20 days[36]. The half-life of IgE secreting plasma cells—which replace circulating IgE—is more contentious, spanning from months to years. Blockage of plasma cell production with the immunotherapeutic drug Dupilumab shows >80% loss of circulating IgE over one year (reviewed in[37]), a slower kinetic than found here. While no other studies have examined SmTAL1-IgE half-life, previous unpublished work found significantly lower titres of schistosome worm antigen (SWA)-specific IgE one year after treatment of Kenyan SAC[34]. Further, *S. haematobium* models developed to investigate antibody isotype switching[29,30] estimated an initial antibody response from short-lived plasma cells of 5–46 days[30] and 3.2–32 days[29], while estimates of the longer-lived antibody response were 9–90 years[30] and 10 months–87 years[29]. The difference in estimates between previous work and ours could reflect biological differences between schistosome species, the modelled mechanism of protective immunity, and other modelling assumptions (e.g., age-exposure patterns and worm life-span). While we do not find that delayed concomitant immunity is necessary to explain immunoepidemiological profiles at endemic equilibrium and 18 months post-treatment in this population, we cannot rule out its importance for the longer-term epidemiology and transmission dynamics of intestinal schistosomiasis.

A principle of helminth epidemiology is that acquired immunity increases the resilience of parasite populations to interventions via the release of immune-mediated density-dependent constraints[11,38]. Previous transmission dynamics modelling of schistosomiasis has demonstrated this explicitly, showing that the loss of acquired immunity during MDA increases rates of reinfection[9,18]. By contrast, our modelling of MDA shows that stronger declines in infection and decreased rates of reinfection occur when immunity is incorporated compared to when it is omitted. This occurs because of the protection against reinfection afforded by SmTAL1-IgE antibodies—which are transiently boosted following the death of adult schistosomes after treatment—but also because the accumulation of protective antibodies during childhood increases the aggregation of worms in SAC, the demographic with the highest coverage of MDA.

Past models have often assumed that cumulative live worms are the source of antigenic stimulation for acquired immunity against schistosomes[9,11,18] but a compelling body of evidence now suggests this role is instead fulfilled by cumulative exposure to dying worms[12–14,17,29–31]. These different sources of immunostimulation will yield tangible differences in projected dynamics. Assuming a live-worm stimulus, reductions in worm burden caused by treatment will cause a faster

decline in protective immunity leading to more rapid rates of reinfection[18]. Assuming dead worms provide the stimulus, worms killed by treatment will boost the immune response, initially reducing rates of reinfection. However, in keeping with previous serological[39,40] and modelling[17] studies, our model also highlights that the immunological boosting effect of praziquantel is transient, both immediately after treatment—due to the relatively short estimated half-life of SmTAL1-IgE—and longer-term due to reductions in infection. Thus, in the long-term, the qualitative effect on transmission dynamics of different sources of immunostimulation will become similar as population immunity is diminished under both mechanisms. Indeed, premature cessation of MDA can result in a rapid rebound in infections, even 'overshooting' pre-treatment levels[17,41].

Our approach to modelling delayed concomitant immunity is necessarily a simplification of the underlying immunological mechanisms and incurs limitations. First, it is possible that our strategy of leveraging the relationship between SmTAL1 and SmTAL3/5 gave insufficient resolution to detect an immune effect. Previous work from Lake Victoria, Uganda, found that of 89 individuals with measureable SmTAL1-IgE titres, only 43% (*n*=38) were SmTAL3-IgE responders, and 19% (*n*=17) SmTAL5-IgE responders[13,34]. If these proportions were similar for our dataset, it might be challenging to find a protective signal—particularly if it were weak. Second, we do not account for a possible counter-balancing effect of IgG4, which is thought to downregulate IgE by competitively binding to the same epitopes[42]. Several studies have reported that the balance of IgE/IgG4 determines the resistance versus susceptibility to reinfection[24,42,43]. Finally, we use a deterministic model which gives a mean-field approximation of transmission dynamics. A stochastic individual-based model would permit individual variability in worm burdens and antibody responses to be captured; albeit this approach would incur considerable technical difficulties in fitting to data. Notwithstanding these limitations, we emphasise the significant utility of the modelling framework presented here, which could be adapted to fit other data or other proposed immune mechanisms.

Future research could seek to design alternative population sampling strategies to better distinguish the two hypotheses represented by the model variants. Since datasets on long-term TAL family IgE dynamics are lacking, it would be helpful to introduce longer-term immunological monitoring of endemic populations. Data collected from such monitoring could then be used in conjunction with longer-term longitudinally-collected parasitological data—such as programmatic data collected during MDA—to better validate and compare the long-term model dynamics. Future modelling studies could also focus on other markers of acquired immunity, including the newly-characterized SmTAL11, which has also been implicated in the generation of cross-reactive IgEs specific to SmTAL3 and SmTAL5[12].

In conclusion, the contributions of exposure versus immunity to schistosome epidemiology, first noted five decades ago[3], remain unresolved. This paper illustrates that disentangling these two processes is challenging even with complete individual-level immunoepidemiological data. We found that model variants incorporating or omitting delayed concomitant immunity could describe

equally well immunoepidemiological patterns of intestinal schistosomiasis before intervention and 18 months after MDA in a highly endemic community of western Uganda. Despite this unresolved uncertainty, our modelling also indicates that the effects of acquired immunity may become apparent after repeated years of MDA and thus immunity should not be discounted from future modelling projections on the effectiveness of schistosomiasis interventions and the feasibility of reaching the WHO 2030 elimination goals.

Materials and Methods

Datset and study population

Details of the data used in this study have been described previously[21–24]. Briefly, a longitudinal reinfection study was conducted in Booma, a fishing village on the eastern shore of Lake Albert, Uganda, highly endemic for *S. mansoni* with an estimated community prevalence in 1998 of 94%[44]. Parasitology, serology, and intensive water-contact observations for 12 hours per day over a 10-month period were conducted, in conjunction with systematic snail surveys, between 1998 and 2000[23]. Baseline data were collected before the introduction of MDA and can, therefore, be assumed to reflect the epidemiology at endemic equilibrium. This is an advantage for the current analysis as it avoids the need to model explicitly the effect of interventions or other secular changes (e.g., environmental or ecological change) which would introduce additional complexity and uncertainty. Following the collection of baseline (pre-treatment) data in May 1998, from July 1998 a randomly sampled subset of the community was treated twice, two weeks apart, with praziquantel at 40 mg/kg of body weight. *S. mansoni* eggs per gram of faeces (epg) and SmTAL1-IgE optical density (OD) were longitudinally measured at follow-up at 5 weeks, 12 months, and 18 months after the second treatment[24]. The sample used in the current study comprises 110 individuals of the Alur ethnic group (the now dominant ethnic group in the Lake Albert region[45]) aged 7–50 years old from whom data were collected on cercarial exposure and a subset of 85 individuals (aged 7–47) with paired data on epg and SmTAL1-IgE OD (Supporting Information, Table S1). At each sampling time point, individual epg data were calculated as the average of two Kato-Katz egg counts, from three stool samples, collected on consecutive days. Data on SmTAL1-IgE ODs were calculated from triplicate repeats using control serum to account for between-plate variation.

Ethics

The original study obtained informed consent from all participants and ethical clearance was granted by the Uganda National Council for Science and Technology (UNCST)[23,24]. The current analysis is in line with the approved study aim of determining the roles of exposure and immunity on levels of infection and associated morbidity.

Transmission dynamics model

We developed a mathematical model in R[46] (using packages *Rcpp*[47], *RcppNumerial*[48] and *RcppEigen*[49]) to describe age- and sex-dependent epg and SmTAL1-IgE antibody OD (Figure 2; www.github.com/gcmilne/SchistoTransmissionModel). The model is based on the population-based deterministic structure originally presented by Anderson and May[4] and more recently in Neves et al.[50] but with the miracidial and cercarial schistosome life-stages compressed into two components of the basic reproduction number, R_0, and additional complexity introduced to model the production and loss of SmTAL1-IgE. Here, we give a brief overview of the model (Figure 2) with a complete derivation given in the Supporting Information.

We model the mean number of schistosomes in $i = 1 \ldots n$ worm compartments within human hosts of age a, sex s, and time t, $W_i(a,s,t)$, the cumulative number of dead schistosomes $D(a,s,t)$, and the average degree of acquired immunity, $I(a,s,t)$, using a set of integro-partial differential equations,

$$\frac{\delta W_1(a,s,t)}{\delta t} + \frac{\delta W_1(a,s,t)}{\delta a} = \frac{R_0\mu_2\psi_1(a,s)\left(\sum_s \eta_s \int_0^\infty \psi_1(a,s)g(a)W(a,s,t)\Phi[W(a,s,t),k(t)]\,da\right)\Theta[I(a,s,t),\omega]}{\rho R_0^\pi (N_1/N_2)\left(\sum_s \eta_s \int_0^\infty \psi_1(a,s)g(a)W(a,s,t)\Phi[W(a,s,t),k(t)]\,da\right) + \mu_2/\mu_1} - n\mu_1 W_1(a,s,t) \quad (1)$$

$$\frac{\delta W_{2\ldots n}(a,s,t)}{\delta t} + \frac{\delta W_{2\ldots n}(a,s,t)}{\delta a} = n\mu_1 W_{i-1}(a,s,t) - n\mu_1 W_i(a,s,t)$$

$$\frac{\delta D(a,s,t)}{\delta t} + \frac{\delta D(a,s,t)}{\delta a} = n\mu_1 W_n(a,s,t)$$

$$I(a,s,t) = \int_0^a e^{-\sigma(a-a')} D(a',s,t-a)$$

Here, N_1/N_2 is the human-to-snail population density, μ_1 and μ_2 are the *per capita* mortality rates of schistosomes and infectious snails respectively, ρ is the schistosome sex ratio (proportion female), and $\psi_1(a,s)$ is a normalized exposure function, with shape matching observed age- and sex-depedent ceracial exposure scores[23] (Figure 1). The function $\Phi[W(a,s,t),k(t)]$ denotes the (monogamous) mating probability[51], where $k(t)$ is the overdispersion parameter of a negative binomial distribution which is assumed to adequately capture the distribution of schistosomes among human hosts[4,52], and which is dynamically affected by MDA (aggregation is transiently increased following rounds of treatment) but is assumed constant for age and sex[53]. The function $\Theta[I(a,s,t),\omega] \in (0,1)$ is the acquired immunity-dependent probability of cercarial establishment,

$$\Theta[I(a,s,t),\omega] = e^{-\omega I(a,s,t)} \quad (2)$$

where parameter ω describes the strength of protection afforded by acquired immunity. Parameter σ is the rate of decay of acquired immunity, such that $12\ \ln(2)/\sigma$ is the antibody half-life in months.

Our apoproach to modelling acquired immunity aligns with previous methodologies[9,18] but uses cumulative dead, not live, worms as the source of antigenic stimuli[13,54].

Model calibration

We calibrated the model with data on epg and SmTAL1-IgE OD. The epg is given by,

$$E(a,s,t) = \lambda W(a,s,t)\Phi[W(a,s,t),k(t)] \quad (3)$$

where λ is the per worm fecundity of mated female schistosomes and $W(a,s,t) = \sum_i^n W_i(a,s,t)$, i.e., the per host total mean worm burden. Note that in the absence of strong evidence for density-dependent fecundity in *S. mansoni*[55] we assume, in line with previous modelling[56], that λ is independent of $W(a,s,t)$. The OD of SmTAL1-IgE antibodies is given by,

$$IgE(a,s,t) = I(a,s,t)\phi \quad (4)$$

where ϕ is a proportionality constant (analogous to λ) that maps acquired immunity to observed OD.

Parameter estimation

We fitted two variants of the model: the 'standard model' in which SmTAL1-IgE is a passive marker of past exposure and has no impact on the probability of cercarial establishment (i.e., $\omega = 0$; eqn. 2, Figure 2), and the 'immunity model', in which SmTAL1-IgE can reduce the probability of cercarial establishment (i.e., $\omega \in (0,1)$; eqn. 2, Figure 2). We employed a Bayesian approach, sampling 100,000 parameter sets from a 6- ('standard model') or 7- ('immunity model') dimensional Latin hypercube, assuming uniform priors for each parameter (Figure 4). For each parameter set, the model was run to endemic stability and the simulated age- and sex-specific epg (eqn. 3) and SmTAL1-IgE OD (eqn. 4) profiles extracted and matched to corresponding data[24]. A likelihood function was derived that accounts for the dependence among pairs of epg and SmTAL1-IgE OD observations made from the 85 indviduals sampled at pre-intervention endemic equilibrium (Supporting Information, *Likelihood function*). Parameter posterior distributions were approximated by selecting parameter sets obtaining the top 1% of log likelihoods[57] (i.e., 1,000 parameter sets), with each set of unique parameter values giving rise to a distinct age- and sex-specific epg and SmTAL1-IgE profile.

Model comparison

We calculated the deviance information criterion (DIC) for each of the two model variants to compare their goodness-of-fits[58]. We calculated the median DIC and 95% credible interval (crI) for each model using 1,000 bootstrap replicates from the parameter posterior distribution, sampling without replacement. The model with the lowest DIC score was assumed to be the most

parsimonious and adequate description of the data (Supporting Information, *Comparing model performance*).

Model prediction

We compared the predictive performance of the two model variants against epg and SmTAL1-IgE OD data collected at 5 weeks, 12 months and 18 months after MDA for each of the 1,000 posterior parameter sets estimated using the pre-intervention data. We modelled MDA as an instantaneous reduction in worm burden in the treated proportion of the population[56] with the magnitude defined by the product of the age-specific treatment coverage and praziquantel efficacy (Supporting Information, *Simulating mass drug administration*). Worms killed by treatment transitioned to the dead worm state, causing treatment to transiently increase SmTAL1-IgE antibodies (eqns. 1, 2, 4; in line with observational data[14,32]). We fixed the efficacy of praziquantel to 95%[59] and, since the whole study cohort was treated[24], set the coverage to 100% across the range of minimum and maximum ages of individuals in the study (7 and 50 years, respectively)[24] and to 0% outside these ages. We quantified the predictive performance of the model variants against the data for each post-treatment time-point[24] by calculating an age- and sex-matched root mean squared error (RMSE) statistic[60] (Supporting Information, *Predictive performance*).

Dynamics through mass drug administration

We compared the longer-term treatment dynamics of the model variants (via median posterior dynamics and 95% crIs) by simulating 10 rounds of annual treatment. Praziquantel coverage was set to 75% in school-aged children (SAC, 5–15 years old), reflecting the WHO 2020 target coverage for this demographic group[1], and 30% in adults (≥16 years old), providing a mean (population structure-weighted) coverage of 50.5% in individuals ≥5 years. These assumptions concorded with community-wide coverage surveys in Mayuge District, which estimated population coverage at 52.6% in 2013[25] and 46.5% in 2016[26], and demographic group-specific coverage at 70.7% in SAC and approximately 25% in individuals ≥20 years[26].

In a sub-analysis, we classified the immunity model simulations into iterations reaching the lowest 10% of epg values after ≥5 years of MDA and iterations in the remainder of the epg distribution. This allowed for the investigation of areas of parameter space associated with effective treatment and—where stubbornly low transmission was maintained—immunity-mediated resilience against elimination.

Acknowledgments

This work could not be realised without the friendly co-operation of the people of Buliisa District. We would also like to acknowledge VCD technicians, especially the late J. Kemijumbi, A. Wamboko, and D. Nionsaba, and A. Babyesiza and N. Okumu for their dedication in leading the

water contact observation team at Lake Albert. We deeply appreciate the field team leadership by Drs F. Kazibwe and E. M. Tukahebwa. The IgE data were generated under the leadership of Prof. D.W. Dunne; SW thanks him for the wealth of immunity data that allowed this work. Dr A. Pinot de Moira is thanked for her tireless work in generating the cercarial exposure scores. Finally, we are most grateful for the late Prof. A. E. Butterworth, Dr. J. H. Ouma, Prof. B. J. Vennervald and A. J. C. Fulford, whose inputs were extremely valuable in shaping the original study design.

Funding Information

GCM, RCO, JPW, MW and SW were supported through the FibroScHot project which is part of the EDCTP2 programme supported by the European Union (RIA2017NIM-1842-FibroScHot). RCO was initially funded by the UK Medical Research Council, UK Doctoral Training Partnership (grant MR/K50127X/1). CW was supported by a Sir Henry Wellcome Postdoctoral Fellowship (224190/Z/21/Z). CW and MGB acknowledge funding from the MRC Centre for Global Infectious Disease Analysis (MR/X020258/1), funded by the UK Medical Research Council (MRC). This UK-funded award is carried out in the frame of the Global Health EDCTP3 Joint Undertaking. MGB and MW also acknowledge funding from the Bill & Melinda Gates Foundation through the NTD Modelling Consortium (grant INV-030046).

Data and Code Availability

The data used to fit the model in this publication have been deposited in a UK Data Service ReShare Repository. Age has been collapsed into 5-year age groups to improve participant anonymity. [dataset]* Oettle, Rebecca C and Pinot de Moira, Angela and Vennervald, Birgitte J and Dunne, David W and Kabatereine, Narcis B and Wilson, Shona (2024). *Revisiting Immunity Versus Exposure in Schistosomiasis: A Mathematical Modelling Study of Delayed Concomitant Immunity, 1998-2000.* [Data Collection]. Colchester, Essex: UK Data Service. 10.5255/UKDA-SN-857172.

The model code is publicly available as an R package at www.github.com/gcmilne/SchistoTransmissionModel.

Figure Legends

Figure 1. Fit of non-linear exposure function (see Supporting methods) to cercarial exposure data (*N*=110 individuals)[23]. Points and error bars show, respectively, the observed means and associated 95% confidence intervals (calculated using 1,000 nonparametric bootstrap samples). Lines and shaded areas show, respectively, the best-fit model estimates obtained via maximum likelihood estimation using a quasi-Newton optimization algorithm, and the modelled 95% confidence intervals (estimated using 1,000 parametric bootstrap samples of parameter values from a multivariate normal distribution parameterized with the variance-covariance matrix of the best-fit model). Note that best-fit model estimates were normalized (to sum to 1) before use in the transmission model such that only the relative shapes and magnitudes of the functional forms influenced model dynamics. See the Supporting Information for further details.

Figure 2. Transmission model structure. The model tracks the mean worm burden of adult *Schistosoma mansoni* divided into $i \in (1, n)$ latent compartments, $W_i(a, s, t)$, across time and host age and sex. The infection dynamics are driven by the force of infection, Λ, which is a function of the vector of model parameters, θ, the age- and sex-specific cercarial exposure, $\psi_1(a, s)$, and the host population structure, $g(a)$ (with age- and sex-dependencies omitted in the figure for brevity). Worms enter compartment W_1, pass between n contiguous compatments at rate $n\mu$ and die after leaving the nth compartment. Eggs are excreted from the host by worms in all compartments (indicated by the grey dashed box) at a rate determined by a constant egg-shedding parameter, λ, and a worm mating probability, Φ (a function of W and the among-host worm overdispersion parameter, k), producing the number of eggs per gram of faeces (epg). Worms that die move to compartment D, which counts the cumulative number of dead worms experienced by hosts. A function, $f(D, \sigma)$, relates this cumulative experience to the acquired immune response, I, by integrating through past age and time while accounting for antibody decay through rate parameter σ. The acquired immune response of compartment I is mapped to a measured IgE optical density (OD) through a constant parameter, φ. A function, $\Theta(I, \omega)$, relates the level of acquired immunity to the probability of cercarial infection establishment; parameter ω determines the level of protection, ranging from none ($\omega = 0$) to increasingly strong ($\omega \to 1$) protection. Note that all compartments and outputs are host age- and sex-specific (not shown here for brevity). Dotted grey arrows represent flows to model outputs that do not impact transmission dynamics. For a full description of parameters and model derivation see the Supporting Information. Figure created with BioRender.

Figure 3. Model fits against pre-treatment data and validation against post-treatment data. Immunoepidemiological outputs—eggs per gram of faeces (epg) and *Schistosoma mansoni* Tegumental Allergen-Like protein 1 immunoglobulin E optical density (SmTAL1-IgE OD)—are presented for the model including ('immunity model'; orange) or excluding ('standard model'; purple) delayed concomitant immunity. In panels **A** and **B**, the first columns show the model fits to baseline (pre-intervention) data (*N*=85 individuals; see also Supporting Information Fig. S2 for an overlaid plot)[24], while subsequent columns show model validation against (without fitting to) post-treatment data collected 5 weeks (*N*=75 individuals), 12 months (*N*=63 individuals), and 18 months (*N*=67 individuals) after the second of two community-wide praziquantel treatments[24]. Points represent the mean age-aggregated data and error bars the associated 95% binomial confidence intervals (calculated using 1,000 nonparametric bootstrap samples). Lines represent the median modelled estimates (50th percentile of simulated outputs) and shaded areas the associated 95% credible intervals (2.5 and 97.5 percentiles). Posterior distributions were approximated by selecting parameter sets obtaining the top 1% of log likelihoods[57] (i.e., 1,000 parameter sets). In line with the study protocol[24], we simulated two treatments with 40 mg/kg body weight of praziquantel, two weeks apart, with 100% coverage over the range of ages of individuals in the study (7–50 years old)[24]. Note that SmTAL1-IgE data were only collected until 5 weeks post-treatment. Panel **C** shows comparative model posterior dynamics (posterior medians and 95% credible intervals) under 10 rounds of annual mass drug administration, with treatment coverage of 75% in school-aged children (5–15 years old)—representing the World Health Organization target for this demographic group[1]—and a nominal 30% in adults (≥16 years), yielding a mean (population-weighted) coverage of 50.5% in line with Ugandan coverage surveys[25,26]. Outputs are presented as host population density- and sex ratio-weighted means, using demographic data sourced from the United Nations[61]. Praziquantel efficacy (egg reduction rate) was set to 95% for all simulations[59].

Figure 4. Summary of the posterior distributions of parameters estimated by fitting the model including ('immunity model') or omitting ('standard model') delayed concomitant immunity to immunoepidemiological data[24]. For each parameter, dots show the median posterior estimate (the top 1% of log likelihoods from 100,000 simulations[57]), whiskers the lower and upper 95% credible interval (crI; the 2.5 and 97.5 percentiles of the posterior distributions), and grey shaded areas the (uniform) prior ranges. Note that the immune protection parameter, ω, was fixed to 0 for the standard model, hence no parameter estimation was performed here. Parameter notation: R_0, basic reproduction number; π, weighting parameter defining asymmetry of transmission (humans-to-snails vs. snails-to-humans); k, among-host worm overdispersion; ω, SmTAL1-IgE mediated protection against cercarial establishment; σ, rate of decay of SmTAL1-IgE antibodies; ϕ, constant

that maps acquired immunity to antibody optical densities; N_1/N_2, human-to-snail population density.

References

1 World Health Organization. Ending the neglect to attain the Sustainable Development Goals: a road map for neglected tropical diseases 2021–2030. Geneva, 2021 https://www.who.int/publications/i/item/9789240010352 (accessed September 18, 2024).

2 GBD 2021 Diseases and Injuries Collaborators. Global incidence, prevalence, years lived with disability (YLDs), disability-adjusted life-years (DALYs), and healthy life expectancy (HALE) for 371 diseases and injuries in 204 countries and territories and 811 subnational locations, 1990–2021: a systematic analysis for the Global Burden of Disease Study 2021. *Lancet* 2024; **403:** 2133–61.

3 Warren KS. Regulation of the prevalence and intensity of schistosomiasis in man: immunology or ecology? *J Infect Dis* 1973; **127**: 595–609.

4 Anderson RM, May RM. Helminth infections of humans: mathematical models, population dynamics, and control. *Adv Parasitol* 1985; **24**: 1–101.

5 Woolhouse ME. On the application of mathematical models of schistosome transmission dynamics. I. Natural transmission. *Acta Trop* 1991; **49**: 241–70.

6 Blackwell AD, Gurven MD, Sugiyama LS, *et al.* Evidence for a peak shift in a humoral response to helminths: age profiles of IgE in the Shuar of Ecuador, the Tsimane of Bolivia, and the U.S. NHANES. *PLoS Negl Trop Dis* 2011; **5**: e1218.

7 Mutapi F, Ndhlovu PD, Hagan P, Woolhouse MEJ. A comparison of humoral responses to *Schistosoma haematobium* in areas with low and high levels of infection. *Parasite Immunol* 1997; **19**: 255–63.

8 Arnold BF, Kanyi H, Njenga SM, *et al.* Fine-scale heterogeneity in *Schistosoma mansoni* force of infection measured through antibody response. *Proc Natl Acad Sci U S A* 2020; **117**: 23174–81.

9 Kura K, Hardwick RJ, Truscott JE, Anderson RM. What is the impact of acquired immunity on the transmission of schistosomiasis and the efficacy of current and planned mass drug administration programmes? *PLoS Negl Trop Dis* 2021; **15**: e0009946.

10 Chan MS, Mutapi F, Woolhouse MEJ, Isham VS. Stochastic simulation and the detection of immunity to schistosome infections. *Parasitology* 2000; **120**: 161–9.

11 Anderson RM, May RM. Herd immunity to helminth infection and implications for parasite control. *Nature* 1985; **315**: 493–6.

12 Oettle RC, Dickinson HA, Fitzsimmons CM, *et al.* Protective human IgE responses are promoted by comparable life-cycle dependent Tegument Allergen-Like expression in *Schistosoma haematobium* and *Schistosoma mansoni* infection. *PLoS Pathog* 2023; **19**: e1011037.

13 Fitzsimmons CM, Jones FM, Pinot de Moira A, *et al.* Progressive cross-reactivity in IgE responses: an explanation for the slow development of human immunity to schistosomiasis? *Infect Immun* 2012; **80**: 4264–70.

14 Black CL, Mwinzi PNM, Muok EMO, *et al.* Influence of exposure history on the immunology and development of resistance to human schistosomiasis mansoni. *PLoS Negl Trop Dis* 2010; **4**: e637.

15 NTD Modelling Consortium Schistosomiasis Group. Insights from quantitative and mathematical modelling on the proposed WHO 2030 goal for schistosomiasis. *Gates Open Res* 2019; **3**: 1517.

16 Kura K, Ayabina D, Hollingsworth TD, Anderson RM. Determining the optimal strategies to achieve elimination of transmission for *Schistosoma mansoni*. *Parasit Vectors* 2022; **15**: 55.

17 Mitchell KM, Mutapi F, Mduluza T, Midzi N, Savill NJ, Woolhouse MEJ. Predicted impact of mass drug administration on the development of protective immunity against *Schistosoma haematobium*. *PLoS Negl Trop Dis* 2014; **8**: e3059.

18 Chan MS, Anderson RM, Medley GF, Bundy DAP. Dynamic aspects of morbidity and acquired immunity in schistosomiasis control. *Acta Trop* 1996; **62**: 105–17.

19 McManus DP, Loukas A. Current status of vaccines for schistosomiasis. *Clin Microbiol Rev* 2008; **21**: 225–42.

20 Hotez PJ, Bottazzi ME. Human schistosomiasis vaccines as next generation control tools. *Trop Med Infect Dis* 2023; **8**: 170.

21 Booth M, Mwatha JK, Joseph S, *et al.* Periportal fibrosis in human *Schistosoma mansoni* infection is associated with low IL-10, low IFN-gamma, high TNF-alpha, or low RANTES, depending on age and gender. *J Immunol* 2004; **172**: 1295–303.

22 Booth M, Vennervald BJ, Kabatereine NB, *et al.* Hepatosplenic morbidity in two neighbouring communities in Uganda with high levels of *Schistosoma mansoni* infection but very different durations of residence. *Trans R Soc Trop Med Hyg* 2004; **98**: 125–36.

23 Pinot de Moira A, Fulford AJC, Kabatereine NB, *et al.* Microgeographical and tribal variations in water contact and *Schistosoma mansoni* exposure within a Ugandan fishing community. *Trop Med Int Health* 2007; **12**: 724–35.

24 Pinot de Moira A, Fulford AJC, Kabatereine NB, Ouma JH, Booth M, Dunne DW. Analysis of complex patterns of human exposure and immunity to schistosomiasis mansoni: the influence of age, sex, ethnicity and IgE. *PLoS Negl Trop Dis* 2010; **4**: e820.

25 Chami GF, Kontoleon AA, Bulte E, *et al.* Profiling nonrecipients of mass drug administration for schistosomiasis and hookworm infections: a comprehensive analysis of praziquantel and albendazole coverage in community-directed treatment in Uganda. *Clin Infect Dis* 2016; **62**: 200–7.

26 Adriko M, Faust CL, Carruthers L V., Moses A, Tukahebwa EM, Lamberton PHL. Low praziquantel treatment coverage for *Schistosoma mansoni* in Mayuge District, Uganda, due to the absence of treatment opportunities, rather than systematic non-compliance. *Trop Med Infect Dis* 2018; **3**: 111.

27 Anderson RM, Turner HC, Farrell SH, Yang J, Truscott JE. What is required in terms of mass drug administration to interrupt the transmission of schistosome parasites in regions of endemic infection? *Parasit Vectors* 2015; **8**: 553.

28 Buck JC, De Leo GA, Sokolow SH. Concomitant immunity and worm senescence may drive schistosomiasis epidemiological patterns: an eco-evolutionary perspective. *Front Immunol* 2020; **11**: 490788.

29 Mitchell KM, Mutapi F, Savill NJ, Woolhouse MEJ. Protective immunity to *Schistosoma haematobium* infection is primarily an anti-fecundity response stimulated by the death of adult worms. *Proc Natl Acad Sci U S A* 2012; **109**: 13347–52.

30 Mitchell KM, Mutapi F, Savill NJ, Woolhouse MEJ. Explaining observed infection and antibody age-profiles in populations with urogenital schistosomiasis. *PLoS Comput Biol* 2011; **7**: 1002237.

31 Pinot de Moira A, Sousa-Figueiredo JC, Jones FM, *et al. Schistosoma mansoni* infection in preschool-aged children: development of immunoglobulin E and immunoglobulin G4 responses to parasite allergen-like proteins. *J Infect Dis* 2013; **207**: 362–6.

32 Fitzsimmons CM, McBeath R, Joseph S, *et al.* Factors affecting human IgE and IgG responses to allergen-like *Schistosoma mansoni* antigens: Molecular structure and patterns of in vivo exposure. *Int Arch Allergy Immunol* 2007; **142**: 40–50.

33 Fitzsimmons CM, Jones FM, Stearn A, *et al.* The *Schistosoma mansoni* tegumental-allergen-like (TAL) protein family: influence of developmental expression on human IgE responses. *PLoS Negl Trop Dis* 2012; **6**: e1593.

34 Oettle RC, Wilson S. The interdependence between schistosome transmission and protective immunity. *Trop Med Infect Dis* 2017; **2**: e1593.

35 Swallow B, Birrell P, Blake J, *et al.* Challenges in estimation, uncertainty quantification and elicitation for pandemic modelling. *Epidemics* 2022; **38**: 100547.

36 Lawrence MG, Woodfolk JA, Schuyler AJ, Stillman LC, Chapman MD, Platts-Mills TAE. Half-life of IgE in serum and skin: consequences for anti-IgE therapy in patients with allergic disease. *J Allergy Clin Immunol* 2017; **139**: 422-428.e4.

37 Ding Z, Mulder J, Robinson MJ. The origins and longevity of IgE responses as indicated by serological and cellular studies in mice and humans. *Allergy* 2023; **78**: 3103–17.

38 Churcher TS, Filipe JAN, Basáñez MG. Density dependence and the control of helminth parasites. *J Anim Ecol* 2006; **75**: 1313–20.

39 Evengard B, Hammarstromi L, Smitht CIE, Johansson SG 0, Linder E. Subclass distribution and IgE responses after treatment in human schistosomiasis. *Clin Exp Immunol* 1988; **73**: 383.

40 Vendrame CM V., Carvalho MDT, Yamamoto CRF, Nakhle MC, Carvalho SA, Chieffi PP. Evaluation of anti-*Schistosoma mansoni* igG antibodies in patients with chronic schistosomiasis mansoni before and after specific treatment. *Rev Inst Med Trop São Paulo* 2001; **43**: 153–9.

41 Mutapi F, Maizels R, Fenwick A, Woolhouse M. Human schistosomiasis in the post mass drug administration era. *Lancet Infect Dis* 2017; **17**: e42–8.

42 Hagan P, Blumenthal UJ, Dunn D, Simpson AJG, Wilkins HA. Human IgE, IgG4 and resistance to reinfection with *Schistosoma haematobium*. *Nature* 1991; **349**: 243–5.

43 Asuming-Brempong EK, Ayi I, van der Puije W, *et al.* Increased ShTAL1 IgE responses post-praziquantel treatment may be associated with a reduced risk to re-infection in a Ghanaian *S. haematobium*-endemic community. *PLoS Negl Trop Dis* 2022; **16**: e0010115.

44 Joseph S, Jones FM, Walter K, *et al.* Increases in human T helper 2 cytokine responses to *Schistosoma mansoni* worm and worm-tegument antigens are induced by treatment with praziquantel. *J Infect Dis* 2004; **190**: 835–42.

45 D'Udine F, Kyasiimire B, Hammill A, Crawford A. Migration and Conservation in the Lake Albert Ecosystem. The International Institute for Sustainable Development. Geneva, 2015 https://www.iisd.org/system/files/publications/migration-conservation-lake-albert-ecosystem-report.pdf (accessed 18 September 2024).

46 R Core Team. R: A Language and Environment for Statistical Computing. 2023. https://www.R-project.org/.

47 Eddelbuettel D, Francois R, Allaire J, *et al.* Rcpp: Seamless R and C++ Integration. 2023. https://cran.r-project.org/web/packages/Rcpp/index.html (accessed March 18, 2024).

48 Qiu Y, Balan S, Beall M, Sauder M, Okazaki N, Hahn T. RcppNumerical: 'Rcpp' Integration for Numerical Computing Libraries. 2023. https://cran.r-project.org/web/packages/RcppNumerical/index.html (accessed March 18, 2024).

49 Bates D, Eddelbuettel D. Fast and elegant numerical linear algebra using the RcppEigen package. *J Stat Softw* 2013; **52**: 1–24.

50 Neves MI, Milne GC, Webster JP, Walker M. Socio-ecological heterogeneity and uncertainty in the elimination of human schistosomiasis. *medRxiv* 2024; : 2024.03.20.24304586.

51 May RM. Togetherness among schistosomes: its effects on the dynamics of the infection. *Math Biosci* 1977; **35**: 301–43.

52 Anderson RM. Populations and infectious diseases: ecology or epidemiology? *J Anim Ecol* 1991; **60**: 1–50.

53 Collyer BS, Anderson RM. Probability distributions of helminth parasite burdens within the human host population following repeated rounds of mass drug administration and their impact on the transmission breakpoint. *J R Soc Interface* 2021; **18**: 20210200.

54 Woolhouse MEJ, Hagan P. Seeking the ghost of worms past. *Nat Med* 1999; **5**: 1225–7.

55 Neves MI, Gower CM, Webster JP, Walker M. Revisiting density-dependent fecundity in schistosomes using sibship reconstruction. *PLoS Negl Trop Dis* 2021; **15**: e0009396.

56 French MD, Churcher TS, Gambhir M, *et al.* Observed reductions in *Schistosoma mansoni* transmission from large-scale administration of praziquantel in Uganda: a mathematical modelling study. *PLoS Negl Trop Dis* 2010; **4**: e897.

57 Beauneé G, Gilot-Fromont E, Garel M, Ezanno P. A novel epidemiological model to better understand and predict the observed seasonal spread of Pestivirus in Pyrenean chamois populations. *Vet Res* 2015; **46**: 86.

58 Spiegelhalter DJ, Best NG, Carlin BP, Van Der Linde A. Bayesian measures of model complexity and fit. *J R Stat Soc Series B Stat Methodol* 2002; **64**: 583–639.

59 Fukushige M, Chase-Topping M, Woolhouse MEJ, Mutapi F. Efficacy of praziquantel has been maintained over four decades (from 1977 to 2018): a systematic review and meta-analysis of factors influence its efficacy. *PLoS Negl Trop Dis* 2021; **15**: e0009189.

60 Wang F, Liu X, Bergquist R, *et al.* Bayesian maximum entropy-based prediction of the spatiotemporal risk of schistosomiasis in Anhui Province, China. *BMC Infect Dis* 2021; **21**: 1171.

61 United Nations. World population prospects, online edition. 2019 https://population.un.org/wpp2019/ (accessed March 18, 2024).

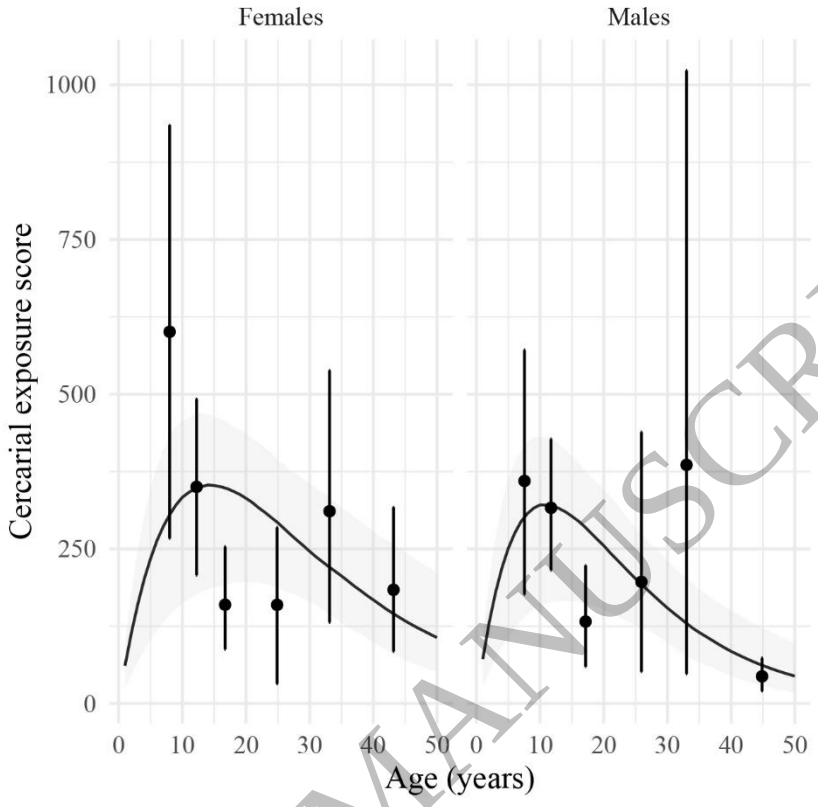

Figure 1
110x107 mm (x DPI)

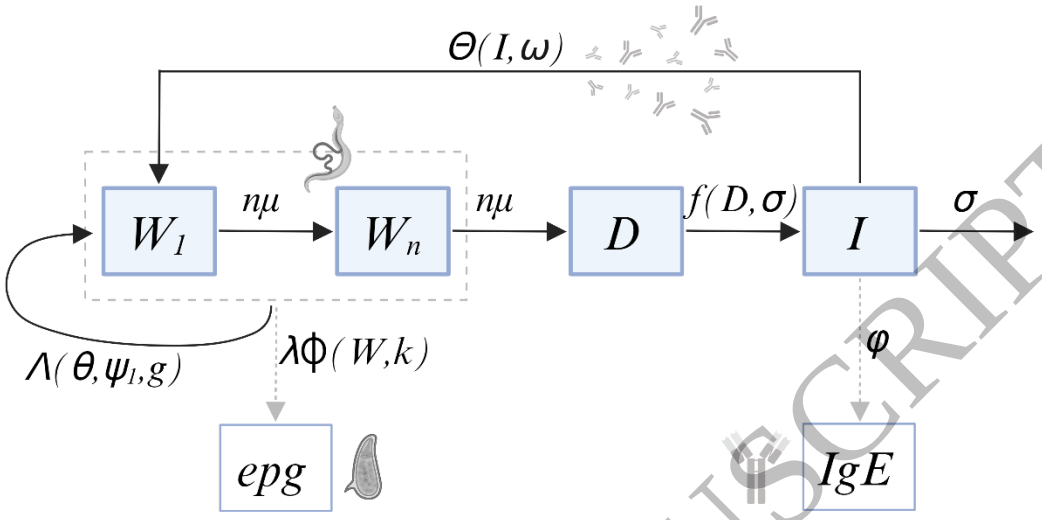

1

2 *Figure 2*
3 *152x76 mm (x DPI)*

4

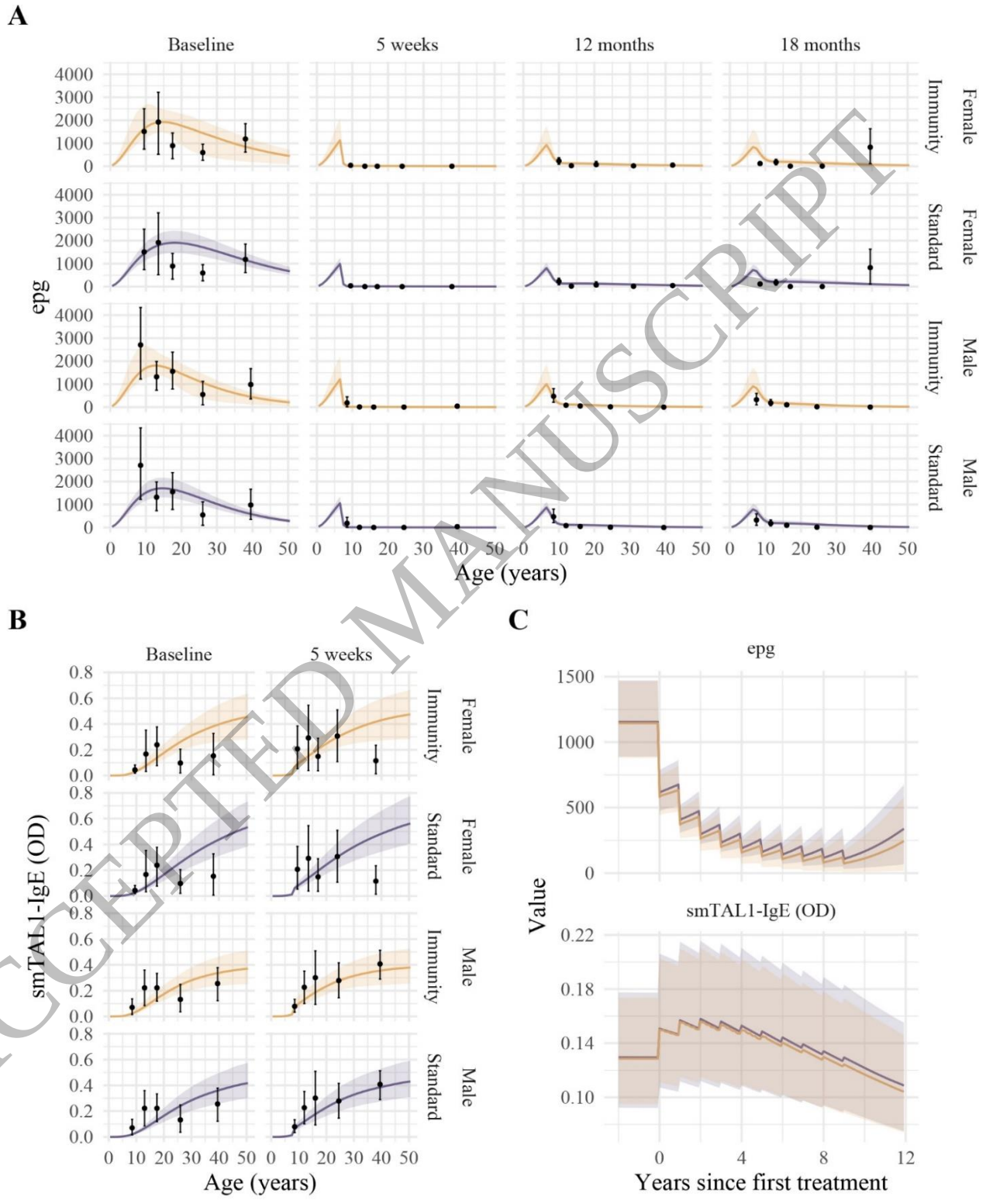

Figure 3
176x216 mm (x DPI)

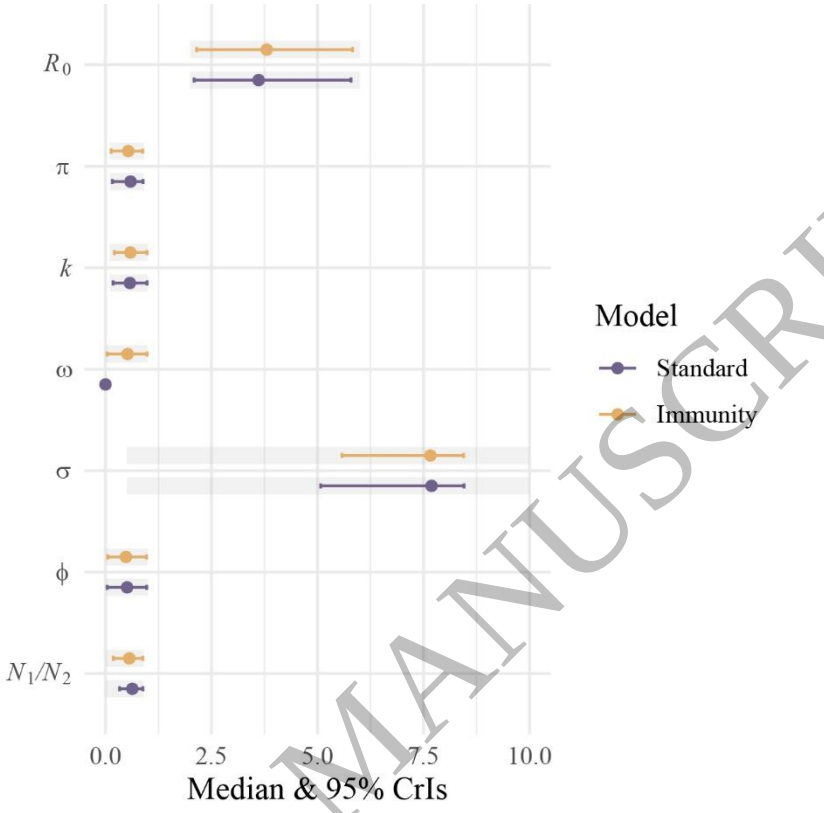

Figure 4
106x107 mm (x DPI)